Magazine of Civil Engineering

ISSN 2712-8172

journal homepage: http://engstroy.spbstu.ru/

DOI: 10.34910/MCE.104.2

Modeling of international roughness index in seasonal frozen area

***L.N. Zhang*[a], *D.P. He*[a*], *Q.Q. Zhao*[b]**

[a] *Northeast Forestry University, Harbin, Heilongjiang Province, China*

[b] *Northeast Agricultural University, Harbin, Heilongjiang Province, China*

** E-mail: hdp@nefu.edu.cn*

Keywords: pavements, deterioration, pavement maintenance

Abstract. In order to solve the international roughness index problem of asphalt concrete pavement in seasonal frozen area, this article takes four typical highways from China's seasonally frozen regions as examples to organize and analyze the geographic location, climatic conditions, structural layer materials and traffic volume of the four roads. Based on the mechanistic-empirical pavement design guide, and by the statistical product and service solutions software for regression analysis, propose IRI correction prediction model of asphalt concrete pavement in the seasonal frozen area and choose IRI measuring values of other highways and the predicted values of IRI prediction model to verify. The result shows that there is a linear relationship between international roughness index, environmental factor, fatigue crack area, transverse crack length and average rut depth. The coefficient of determination R^2 is 0.999, the adjusted R^2 is 0.999, the significance level is 0, and the regression model is effective. The values corresponding to modified model, environmental factor, fatigue crack area, transverse crack length and average rut depth indicators are 0.004, 0.074, 0.143 and 51.563 respectively; The IRI predicted value of the modified model is closer to the measured value than that of the traditional prediction model. The research results are of great significance for the international roughness index prediction of an asphalt concrete pavement in a seasonal frozen area.

1. Introduction

In order to reduce the impact of road surface roughness on driving comfort and safety in the seasonal frozen area, and to solve the impact of road surface on driving safety and road life, the international roughness index needs to be modeled. Since the international roughness index is an important indicator reflecting the road function and evaluating the road performance, the international roughness index prediction model of the asphalt pavement in the seasonal frozen area is established based on the parameters of the asphalt pavement structure, climatic conditions and traffic conditions in the seasonal frozen area. This model is of significant importance for the evaluation of asphalt pavement maintenance in the seasonal frozen area.

At present, the research time of international roughness index prediction at home and abroad is still short, and all of them are research biases to analyze the trend and detection methods of international roughness index. M. Mubaraki [1] establishes the relationship between the International Roughness Index (IRI) and road damage (including cracking, rutting and scattering), but the study is based on the climatic characteristics of Saudi Arabia; S.A. Arhin et al. [2] is based on 2-year IRI-PCI data. The model was developed to predict the relationship between IRI and PCI by functional classification for the pavement type in the Colombian region, but the relationship between IRI and PCI has no guiding significance for the prediction of the IRI model; P. Múčka [3] addresses the main problems in developing countries and some common problems that usually exist on secondary road networks, but there is no distinction between the degree of serious damage; J.P. Bilodeau et al. [4] uses the simulated heavy-duty wheel load response to calculate the dynamic load factor, and establishes the relationship between vehicle axle load and IRI, but the study did not consider the impact of climate and other factors on IRI. S.A. Arhin et al. [5] compares only

the methods of using IRI in US states with those used in non-US countries. M.I. Hossain et al. [6] is based on the neural network-based flexible pavement international flatness index. The analysis is only aimed at wet, frozen, wet, non-frozen and dry non-frozen climate zones. In addition, the neural network has the disadvantages of easy convergence and so on. The model has limitations. M.J. Khattak et al. [7] studied the international flatness index model of flexible base and pavement HMA overlays. The research section is based on Louisiana. The model itself is subject to environmental factors and it is notfurther aimed at the climate characteristics of the seasonal frozen zone. Note that the model is only for flexible base and pavement HMA overlays. In summary, the domestic and international research still lacks the establishment of the international roughness index model for the seasonal frozen area. Therefore, we establish an international roughness index prediction model for asphalt pavement that is suitable for the climate characteristics of the seasonal frozen area, which can fill the blank of the international roughness index prediction of the asphalt pavement in the seasonal frozen area.

2. Methods

The National Cooperative Highway Research Project (NCHRP) and the American National Association of Highway Transportation Administrators (AASHTO) have conducted several years of investigation and collated the observation results of long-term pavement performance distributed in more than 2,200 test sections in various states in the United States, which published Mechanistic-Empirical Pavement Design Guide in 2004, abbreviated as MEPDG [8–11]. It calculates stress and strain [12–13] of pavement structures by means of mechanical methods, based on climatic conditions and material properties of each structural layer, and bridges the gap between laboratory tests and actual road performance [14], based on empirical method and design. The prediction model is shown in formula 1. IRI is affected by the comprehensive influence of fatigue crack area, lateral crack length, rut depth, and environmental factors on the asphalt pavement. These four factors form a linear relationship [15]. The following content of the International Roughness Index is abbreviated as IRI for short.

After years of research, AASHTO in the United States has derived the IRI prediction formula 1 for asphalt pavements in the local MEPDG in the United States:

$$IRI = IRI_0 + 0.015(SF) + 0.400(FC_{Total}) + 0.0080(TC) + 40.0(RD) \quad (1)$$

where IRI_0 is Initial IRI after construction (in/mile);

SF is Environmental factor;

FC_{Total} is Fatigue crack area, a percentage of total lane area;

TC is Transverse crack length (including reflection of lateral cracks in existing HMA pavement) (ft/mile);

RD is Average rut depth (in).

$$SF = Age\left[0.02003(PI+1) + 0.007947(Precip+1) + 0.000636(FI+1)\right] \quad (2)$$

where Age is Pavement age (year);

PI is Percentage plasticity index of soil;

$Precip$ is Average annual rainfall or snowfall (in);

FI is Annual average freezing index (d).

According to the research in the existing literature [16], IRI is significantly affected by FCTotal, TC, and RD, and the linear relationship is obvious. In order to further verify, in the IRI prediction model of asphalt pavement in MEPDG, whether there is a linear relationship between IRI and SF in the seasonal frozen area, and the climate characteristics of the seasonal frozen area are fully covered. In the area of the seasonal frozen area, four typical highwaysare selected, namely the Jian-Ji Highway (Yanggang to Mishan Section) in Hulin City, Heilongjiang Province, China, hereinafter abbreviated as the Jian-Ji Highway; Zhang-Shi Highway (Zhangjiakou Section), Zhangjiakou City, Hebei Province, China, hereinafter abbreviated as Zhang-Shi Highway; Lian-Huo National Highway (Kuitun-Wusu Section) in Wusu City, Xinjiang Uygur Autonomous Region, China, hereinafter abbreviated asLian-Huo National Highway; 110 National Highway (Hubao section), Hohhot City, Inner Mongolia, China, hereinafter abbreviated as 110 National Highway, as shown in Fig. 1.

In Fig. 1, the four roads selected in the article are evenly distributed in China's seasonal frozen soil regions, and the latitude and longitude differences are large, which can reflect the climatic characteristics

of China's seasonal frozen soil regions more comprehensively. The seasonal freezing area in China is characterized by severe freezing in winter and warm and thawing in summer. The freezing and thawing cycle of asphalt concrete pavement in seasonal freezing area is very significant.

Figure 1. Geographical location of a typical highway.

To further verify the impact of SF on IRI, relevant statistical data for four typical highways in 2015 are collected, as shown in Table 1. From Table 1, it can be seen that the difference between the maximum temperature and the minimum temperature of the city where the Jian-Ji Highway among the four typical highways is 67 °C, and the minimum temperature difference between the Jian-Ji Highway and the Zhang-Shi Highway is 16 °C. There are significant differences in temperature characteristics among the four highways. In Table 1, the road age is within 7 years, and the difference in service life is small; the type of subgrade soil is sandy soil or gravel soil (According to China's Highway Subgrade Design Code JTG D30-2004, the subgrade can be divided into four categories: dry, medium wet, wet, and excessively wet, based on the dry and wet states. The maximum particle size of sandy soil and gravel soil is less than 150 mm). The number of maximum freezing-thawing cycles and the number of minimum freezing-thawing cycles are significantly different, reaching 51 times. The winter humidity of the subgrade soil is mainly concentrated between 8-11 %. Because the Lian-Huo National Highway is located in northwestern China, with drought and little rain all the year round, and the total rainfall is only 185 mm, the winter humidity of the subgrade soil is only 8 %.

Table 1. Basic information of typical roads.

Highway name	Highway age	Latitude and longitude	Winter humidity of subgrade soil	Subgrade soil type	Freezing-thawing cycles	Total annual precipitation (including snowfall) (mm)	Maximum temperature (°C)	Minimum temperature (°C)
Jian-ji Highway	5	North latitude 45.23 East longitude 132.11	10 %	Dry,Sandy soil	112	312	34	-33
Zhang-shiHighway	6	North latitude 40.82 East longitude 114.88	11 %	Dry,Gravelly soil	61	460	36	-17
Lian-huo National Highway	7	North latitude 44.45 East longitude 84.62	8 %	Dry,Gravelly soil	87	185	40	-24
110 National Highway	7	North latitude 40.48 East longitude 111.41	10 %	Dry,Sandy soil	103	344	32	-17

In order to analyze the differences in temperature, average annual freezing index, and average annual precipitation of the four highways, monthly average temperature curves, freezing depth curves, and precipitation distribution curves corresponding to the highways are drawn, as shown in Fig. 2 – 4. Because the temperatures below 0 °C from October of each year to March of the following year appear in seasonal frozen soil regions, a complete freezing-thawing process is selected from October of each year to October of the following year. It can be seen from Fig. 2 that the month with the largest monthly average temperature difference among the four highway cities is January 2017. The monthly average temperature difference between the Jian-Ji Highway and the Zhang-Shi Highway is 9.5 °C, and the temperature difference is 2.46 times. The month with the lowest monthly average temperature difference among the four highway cities appeared in October 2017. The monthly average temperature difference between the Lian-Huo National Highway and the Jian-Ji Highway was 3 °C, and the temperature difference is 1.47 times.

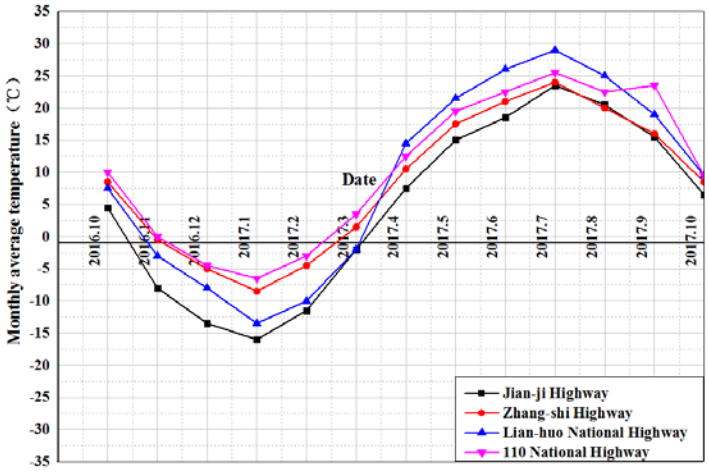

Figure 2. Monthly mean temperature curve of a typical highway.

Fig. 3 is the freezing-thawing depth curve of four typical roads. Since the freezing-thawing time of the highway in the seasonal frozen area is from October of each year to April of the following year, from May 2007 to September 2007, the freezing-thawing depth of the four curves is basically 0 cm. The maximum freezing depth of all four typical highways appeared in February 2017. The largest freezing depth is the Jian-Ji Highway in northeastern China, with a maximum freezing depth of 216 cm, which is followed by Lian-Huo National Highwayin northwestern China, with maximum freezing depth of 161 cm. The third is the 110 National Highway in northern China, with maximum freezing depth of 149 cm, and the smallest freezing depth is the Zhang-Shi Highway in northern China, with the maximum freezing depth of 109 cm. The difference between the maximum freezing depth and the minimum freezing depth is 105 cm. Through analyzing the reason, because in February 2017, the temperature difference between Jian-Ji Highway and Zhang-Shi Highway was 3.83 times, and the difference in precipitation was 2.5 times, under the the coupling of precipitation and temperature, there is a significant difference in freezing depth.

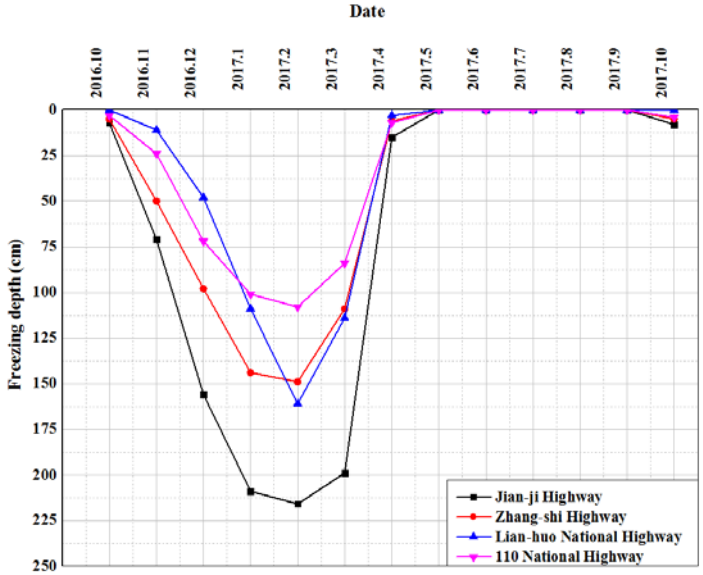

Figure 3. Freezing depth curve of a typical highway.

Fig. 4 shows the precipitation distribution curves of four typical highways from January to December 2017. All four highways have the highest rainfall season of the year in July, among which Jian-Ji Highway is the largest and Lian-Huo National Highway is the smallest. The month when the maximum precipitation occurred also accorded with the actual characteristics of climate precipitation in the seasonal frozen area. The highway with the largest precipitation in the year was Jian-Ji Highway, whose annual precipitation is 393 mm. It accounted for 4.84 %, 80.5 %, 10.43 %, and 4.58 % of the annual precipitation, respectively in spring, summer, autumn and winter. The precipitation of the Zhang-Shi Highway is 388.8 mm, and it accounted for 16.25 %, 62.53 %, 19.11 %, and 2.11 % of the annual precipitation, in spring, summer, autumn and winterrespectively. The precipitation of the Lian-Huo National Highway was 161.9 mm, and it accounted for 32.06 %, 33.23 %, 23.16 %, and 11.55 % of the annual precipitation, in spring, summer, autumn and winterrespectively. The precipitation of the 110 National Highway was 380.8 mm, and it accounted for 13.6 %, 63.2 %, 20.7 %, and 2.5 % of the annual precipitation, in spring, summer, autumn and winterrespectively. It can be seen from Fig. 4 that January-March 2017 and October-December 2017 were periods when the rainfall of four typical highways was relatively small. The reason was that the four highways had successively entered winter.

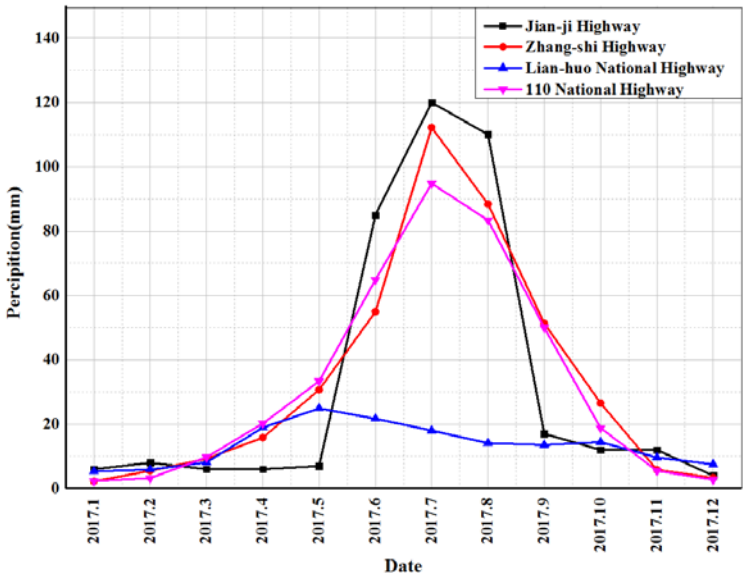

Figure 4. Distribution curve of precipitation of typical roads.

In order to further analyze the impact of temperature, average annual freezing index, and average annual rainfall on IRI, the IRI curve corresponding to four typical highways is established, as shown in Fig. 5. In Fig. 5, the IRI values of the four expressways change with time, and the change law is a linear increase. The three stages of rapid IRI slope change were November-December 2016, June-July 2017, and November-December 2017. The stage maximum appeared first in December 2016, July 2017, and December 2017. From the analysis of the reasons, it can be seen from Fig. 3 that in December 2017, the freezing depth of the four highways reached the maximum, and the soil thawing rate corresponding to the four highways was more than 93.5 %, and the number of freezing-thawing cycles reaches a peak. Under the repeated action of external loads, the smoothness index of the road surface decreases; as shown in Fig. 4, it was the highest rainfall of the four highways in July 2017. At the time of concentration, under the effect of external load, abundant rainwater was poured from the gaps in the road surface, which caused the flatness index of the road surface to decrease. From December 2016 to June 2017, and from August to November 2017, the changes in IRI values were relatively flat. The change slope of the Jian-Ji Highway is significantly higher than that of the other three highways. The reasons were that the annual average temperature of the area where the Jian-Ji Highway was located can vary up to 39.5 °C, the freezing depth can reach 216 cm, and the number of freeze-thaw cycles can be 116 times. According to the above analysis, it can be known that the temperature, average annual freezing index, and average annual rainfall and other factors that constitute SF have positive and linear effects on IRI.

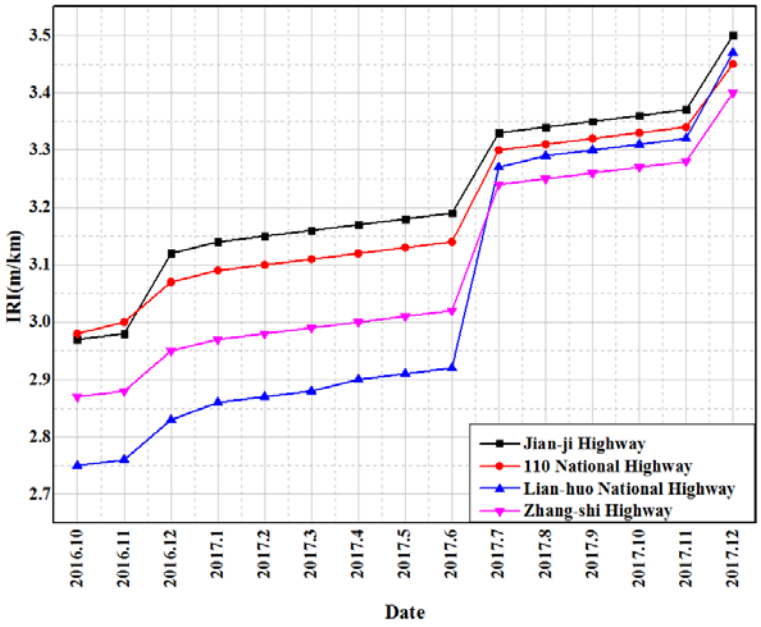

Figure 5. IRI curve of typical highway.

3. Results and Discussion

According to the analysis above, there is a linear relationship among IRI, SF, FCTotal, TC, and RD, and linear regression is performed in combination with field measured data to solve the correlation coefficient R^2. The measured data of the regression are from measured data of road surface IRI, 600 in total, of Jian-Ji Highway (Yanggang to Mishan Section) in Heilongjiang Province, China, Zhang-Shi Highway (Zhangjiakou Section) in Hebei Province, China, and Lian-Huo National Highway (Quitun-Wusu section), Xinjiang Uygur Autonomous Region, China and 110 National Highway (Hubao section), Inner Mongolia Autonomous Region, the four typical roads during 5 years from 2014 to 2018, which were used as the dependent variables of the regression model; combined with the above content, the measured values of SF, FCTotal, TC, and RD of four roads including Jian-Ji Highway (Yanggang to Mishan Section) in Heilongjiang Province, China, Zhang-Shi Highway (Zhangjiakou Section) in Hebei Province, China, and Lian-Huo National Highway (Quitun-Wusu section), Xinjiang Uygur Autonomous Region, China and 110 National Highway (Hubao section), Inner Mongolia Autonomous Region are used as the independent variables of the regression model.

The regression method uses "Statistical Product and Service Solutions" software for linear regression [17–22]. The steps of regression are as follows. First, observe the statistical relationship between the variables through the scatter plot. Through the above analysis, determine the linear relationship of the shape of the regression curve, and get a linear function that reflects the fit, which is shown in Table 2. R^2 is obtained before and after adjustment. Secondly, due to the existence of sampling randomness, the estimated regression equation may not be a true reflection of the quantitative relationship between the population of things. Therefore, it is necessary to perform various tests on the regression equation and display the relevant characteristics between the parameters data to determine whether the equation truly reflects the statistical relationship between the population of things, and get the Anovab of the regression model, as shown in Table 3. Then, by using the sample data under certain statistical fitting criteria, each parameter in the regression model is estimated, and a definitive regression equation is obtained, as shown in Table 4; finally, a colinear diagnosis is performed by the regression equation, as shown in Table 5. In the regression model, V1 represents IRI, V2 represents SF, V3 represents FC Total, V4 represents TC, and V5 represents RD.

In Table 2, the value of R^2 is 0.999. R^2 represents the determinant coefficients of the dependent variable IRI and the independent variables SF, FC Total, TC, and RD. The more the value of R^2 approaches 1, the higher the fit degree of the linear regression equation is. The number of independent variables will affect the value of R^2. In order to prevent the goodness of fit from being affected by the number of independent variables, R^2 needs to be adjusted. The adjusted R^2 is the ratio of the mean square error, and the adjusted R^2 is 0.999. The more the result is close to 1, the more the value is closer to 1, the better the fit degree of the regression equation is. Among them, the standard estimation error of the regression equation is only 0.10885, so it is concluded that the regression equation has a higher degree of good fit, and the part that the model can express IRI accounts for 99.9 %.

Table 2. Summary of regression models.

R^2	Adjusted R^2	Standard estimated error
0.999	0.999	0.10885

Table 3 is used to test the multiple linear regression equation by using the analysis of variance method. The table is used to test the significance of the regression equation. Table 3 shows that the data with relevant characteristics are F, significance, and sum of regression squares. The statistic F is the ratio of the square of the average regression to the sum of the squares of the average residuals. If the value of F is larger, it means that the influence of SF, FC Total, TC, and RD on IRI is much greater than that of random factors on IRI; if the significance value, Sig, is smaller, indicate that the linear equation regression is obvious, the goodness of fit is good, and the significance level should be less than 0.05. If the F value is too small, it means that the influence of the above four variables on IRI is very poor, and the fitted regression line is meaningless. The F value must obey the statistical distribution in degrees of freedom. The total IRI of the linear regression model is 19.544, the regression square is 18.893, the regression mean square is 4.723, the residual square is 0.652, and the residual mean square is 0.012. The F value in the table is very large, whose value is 398.632, and the significance value Sig. is 0, which is less than 0.05. It indicates that the four variables have a great impact on IRI, which is much greater than the impact of random factors on IRI;so the straight line is meaningful. There is a significant linear relationship between the IRI of the F test and SF, FCTotal, TC, and RD, and a linear model can be established. Through the above analysis, it can be determined that the linear regression of IRI as the dependent variable and SF, and FC Total, TC, and RD as independent variables is still valid in the seasonal frozen area [23]. In order to further solve the weights corresponding to SF, FC Total, TC, and RD, the regression model coefficients are solved by using SPSS.

Table 3. Anova[b] of the regression model.

Model		Sum of square	Degree of freedom	Mean square	F	Significance
1	Return	18.893	4	4.723	398.632	0
	Residual	0.652	55	0.012		
	Total	19.544	59			

In Table 4, the non-standardized coefficient B represents the coefficient of each variable, and the corresponding coefficients of SF, FC Total, TC, and RD are 0.04, 0.074, 0.143, and 51.563. The value 0.408 corresponding to IRI0 represents the initial constant corresponding to the regression equation. In Table 4, the confidence intervals of the four variables in the linear equation do not include 0, which proves that the four variables are statistically significant. It can be seen that the linear relationship between the four variables and the IRI is obvious, so these four variables must be retained in the equation which can not be excluded. The magnitude of the absolute value of the standardized partial regression coefficient represents the impact of the four variables on the IRI. The standardized partial regression coefficients are all positive numbers, indicating that the variables are positively correlated with the IRI.

Table 4. Regression model coefficients[a].

						B's 95.0 % confidence interval	
Parameter	Partial regression coefficient	Partial regression coefficient standard error	Standardized partial regression coefficient	t	Significance	Lower limit	Upper limit
IRI_0	0.408	0.133		3.061	0.003	0.141	0.676
SF	0.004	0.015	0.008	3.286	0.076	0.027	0.035
FC_{Total}	0.074	0.011	1.853	7.055	0	0.053	0.095
TC	0.143	0.021	1.652	6.837	0	0.184	0.101
RD	51.563	30.132	0.759	8.349	0	0.045	0.096

To avoid the problem of collinearity among the four variables, it is necessary to use SPSS software to diagnose the collinearity of the model. In order to fully consider the four independent variables and conduct a comprehensive analysis by using stepwise regression method, the order by which the diagnostics are entered in sequence are SF, FCTotal, TC, and RD. All variables are not excluded. Table 5 shows the analysis results of collinear diagnosis.

In Model 1, IRI is the dependent variable, and SF, FCTotal, TC, and RD are independent variables to form a quaternary linear function. According to the model, all variables and constant terms are positive numbers and passed the variable test, which is consistent with the actual situation. From the analysis results in Table 5, it can be concluded that more than 90 % of the variance contribution comes from itself. If the eigenvalues in the table are similar and close to 0, it indicates that the commonality between the four independent variables is serious. In Table 5, the maximum eigenvalue is 4.180 and the minimum is 0.002, and these eigenvalues are different. Therefore, it can be concluded that there is no colinearity problem among the four variables. If the value of the condition index in the table is greater than 15, it means that there may be collinearity. If the value of the condition index is greater than 30, it indicates that the problem of collinearity is serious. In Table 5, the value of the maximum condition index is 8.424, which is far less than 15. From the above analysis, it can be concluded that there is no problem of multicollinearity in the international flatness index model of seasonally frozen regions.

Table 5. Collinear diagnosis.

					Variance ratio			
Model	Dimension	Eigenvalues	Conditional index	Constant	V_2	V_3	V_4	V_5
	1	4.180	1.000	0	0.02	0	0	0
	2	0.501	2.888	0	0.86	0	0	0
1	3	0.314	3.650	0.01	0.08	0	0	0
	4	0.004	2.882	0.69	0	0.01	0.19	0.73
	5	0.002	8.424	0.29	0.04	0.81	0.81	0.27

Based on the above analysis, the international roughness index model in the seasonalfrozen area is proposed as:

$$IRI = 0.408IRI_0 + 0.004(SF) + 0.074\left(FC_{Total}\right) + 0.143(TC) + 51.563(RD) \quad (3)$$

In order to test the accuracy of the prediction results of the prediction model, the test sections of the other five highways in the seasonal frozen area are selected as the verification sections, as shown in Fig. 6. The following 5 roads in December 2018 are verified by the predicted and measured IRI values, as shown in Fig. 7-11, which are 20 test sections of Sui-Man Highway (K550+750~K569+750) in Heilongjiang Province, China, and the 20 test sections of Qinggang-Zhenxiang Highway (K013 + 110 ~ K032 + 110) in Heilongjiang Province, China, 21 test sections of Shen-Da Highway (K183 + 300 ~ K203 + 300) in Liaoning Province, China, 16 test sections of S201 Highway (K223 + 000 ~ K238 + 000) in Xinjiang Uygur Autonomous Region, China, and 15 test sections of 110 National Highway (K574 + 000 ~ K588 + 000) in Inner Mongolia Autonomous Region, China, as shown in 7-11. In Fig. 7–11, the curve change table is drawn based on the field measured IRI value, the predicted IRI value of the international flatness index model of the seasonal frozen area, and the predicted value of the traditional IRI model. The abscissa is the station number of the site section, and the ordinate is IRI value. Compared with the traditional IRI prediction model, the IRI value predicted by the international flatness index model of the seasonal frozen area is closer to the IRI value measured in the field, and the error rate is within 3 %. The above analysis verifies the validity of the IRI results predicted by the international flatness index model of the seasonal frozen area.

Figure 6. Verify the geographic location of the road.

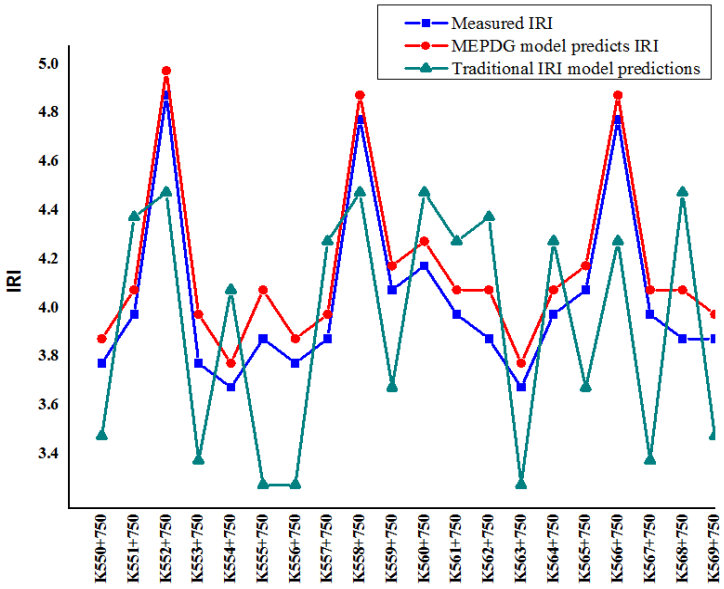

Figure 7. IRI comparison of the Sui-Man Highway.

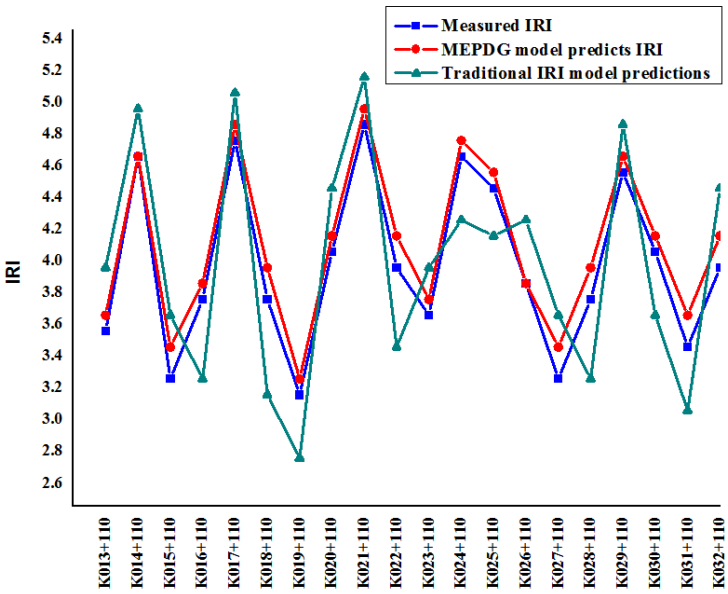

Figure 8. IRI comparison of Qinggang-Zhenxiang Highway.

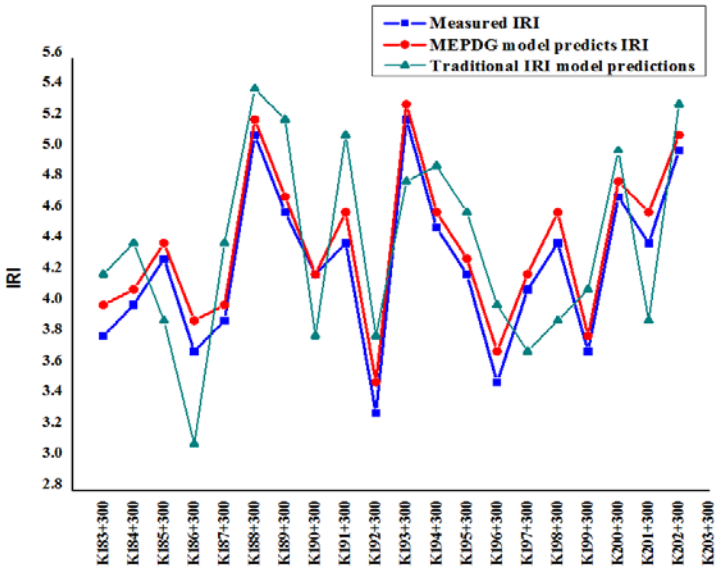

Figure 9. IRI comparison of the Shen-Da Highway.

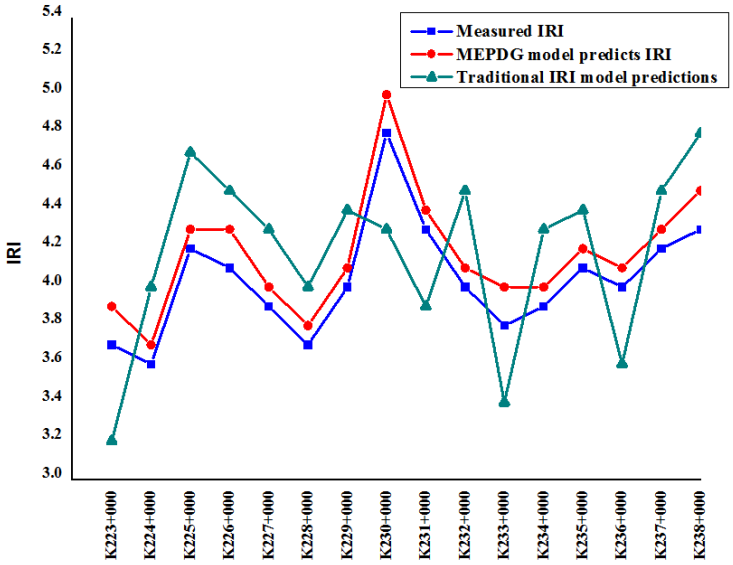

Figure 10. IRI comparison of the S201 Highway.

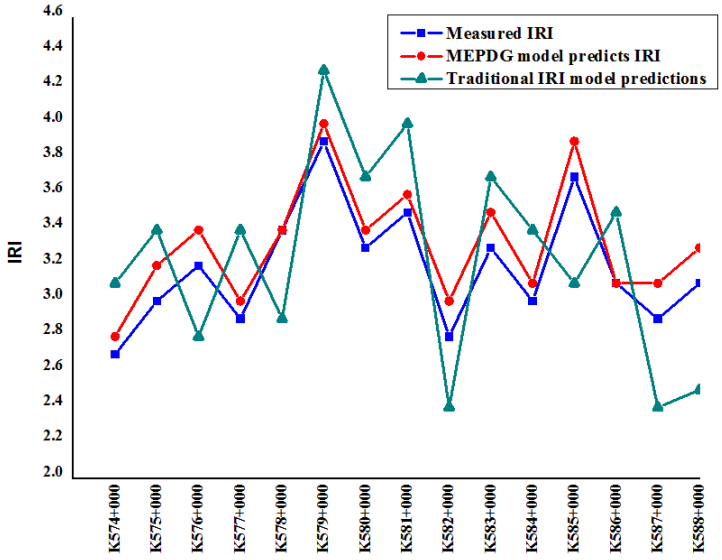

Figure 11. IRI comparison of the 110 National Highway.

4. Conclusion

1. By using SPSS linear regression, the prediction coefficient R^2 is 0.999, the adjusted R^2 is 0.999, the F value is 398.632, and the significance level is 0, which is less than 0.05. It indicates that the regression model has a significant effect.

2. The IRI prediction model of asphalt concrete pavement in the seasonal frozen area is proposed. There is a linear relationship between IRI and the environmental factor, fatigue crack area, transverse crack length and average rut depth, and the values of the four variables are 0.004, 0.074, 0.143 and 51.563 respectively.

3. There is no multicollinearity in the model of the international roughness index of the seasonal frozen area. In the SPSS analysis, the maximum eigenvalues of the four variables are 4.180, the minimum one is 0.002, and the eigenvalues are different. The maximum condition index is 8.424, which is much less than 15.

4. The prediction accuracy of the international roughness index model in the seasonal frozen area is high. In the same time period, choose five highways to compare the predicted value of IRI, the measured IRI value and the traditional predicted IRI value. The results show that the IRI prediction accuracy of the seasonal frozen area international roughness index model is higher than that of other models.

References

1. Mubaraki, M. Highway subsurface assessment using pavement surface distress and roughness data. 8th International Conference on Maintenance and Rehabilitation of Pavements, MAIREPAV 2016. 9(5). Pp. 393–402. DOI: 10.3850/978-981-11-0449-7-329-cd
2. Arhin, S.A., Williams, L.N., Ribbiso, A., Anderson, M.F. Predicting Pavement Condition Index Using International Roughness Index in a Dense Urban Area. Journal of Civil Engineering Research. 2015.5(1). Pp. 10–17. DOI: 10.5923/j.jce.20150501.02
3. Sandra, A.K., Sarkar, A.K. Development of a model for estimating International Roughness Index from pavement distresses. International Journal of Pavement Engineering. 2013. 14(8). Pp. 715–724. DOI: 10.1080/10298436.2012.703322
4. Bilodeau, J.P., Gagnon, L., Doré, G. Assessment of the relationship between the international roughness index and dynamic loading of heavy vehicles. International Journal of Pavement Engineering. 2017. 18(8). Pp. 693–701. DOI: 10.1080/10298436.2015.1121780
5. Múčka, P. International Roughness Index specifications around the world. Road Materials and Pavement Design. 2017. 18(4). Pp. 929–965. DOI: 10.1080/14680629.2016.1197144
6. Hossain, M.I., Gopisetti, L.S.P., Miah, M.S. International roughness index prediction of flexible pavements using neural networks. Journal of Stomatology. 2019. 145(1). DOI: 10.1061/JPEODX.0000088
7. Khattak, M.J., Nur, M.A., Bhuyan, M.R.U.K., Gaspard, K. International roughness index models for HMA overlay treatment of flexible and composite pavements. International Journal of Pavement Engineering. 2014. 15(4). Pp. 334–344. DOI: 10.1080/10298436.2013.842237
8. Mogawer, W.S., Austerman, A.J., Daniel, J.S., Zhou, F., Bennert, T. Evaluation of the effects of hot mix asphalt density on mixture fatigue performance, rutting performance and MEPDG distress predictions. International Journal of Pavement Engineering. 2011. 12(2). Pp. 161–175. DOI: 10.1080/10298436.2010.546857
9. Li, Q., Xiao, D.X., Wang, K.C.P., Hall, K.D., Qiu, Y. Mechanistic-empirical pavement design guide (MEPDG): A bird's-eye view. Journal of Modern Transportation. 2011. 19(2). Pp. 114–133. DOI: 10.3969/j.issn.2095-087X.2011.02.007
10. Caliendo, C. Local calibration and implementation of the mechanistic-empirical pavement design guide for flexible pavement design. Journal of Transportation Engineering. 2012. 138(3). Pp. 348–360. DOI: 10.1061/(ASCE)TE.1943-5436.0000328
11. Tarefder, R., Rodriguez-Ruiz, J.I. Local calibration of MEPDG for flexible pavements in New Mexico. Journal of Transportation Engineering. 2013. 139(10). Pp. 981–991. DOI: 10.1061/(ASCE)TE.1943-5436.0000576
12. Zhang, C., Wang, H., You, Z., Ma, B. Sensitivity analysis of longitudinal cracking on asphalt pavement using MEPDG in permafrost region. Journal of Traffic and Transportation Engineering (English Edition). 2015. 2(1). Pp. 40–47. DOI: 10.1016/j.jtte.2015.01.004
13. Saha, J., Nassiri, S., Bayat, A., Soleymani, H. Evaluation of the effects of Canadian climate conditions on the MEPDG predictions for flexible pavement performance. International Journal of Pavement Engineering. 2014. 15(5). Pp. 392–401. DOI: 10.1080/10298436.2012.752488
14. Allan Reese, R. R for SAS and SPSS Users. Journal of the Royal Statistical Society: Series A (Statistics in Society). 2009. 172(3). Pp. 697–698. DOI: 10.1111/j.1467-985x.2009.00595_7.x
15. Hayes, A.F., Matthes, J. Computational procedures for probing interactions in OLS and logistic regression: SPSS and SAS implementations. Behavior Research Methods. 2009. 41(3). Pp. 924–936. DOI: 10.3758/BRM.41.3.924
16. Gulfam-E-Jannat, Yuan, X.X., Shehata, M. Development of regression equations for local calibration of rutting and IRI as predicted by the MEPDG models for flexible pavements using Ontario's long-term PMS data. International Journal of Pavement Engineering. 2016. 17(2). Pp. 166–175. DOI: 10.1080/10298436.2014.973024
17. Wang, H., Rosner, G.L., Goodman, S.N. Multiple Regression Using SPSS. Clinical Trials. 2016. 13(6). Pp. 621–631. DOI: 10.1177/1740774516649595
18. SPSS survival manual: a step by step guide to data analysis using IBM SPSS. Australian and New Zealand Journal of Public Health. 2013. 37(6). Pp. 597–598. DOI: 10.1111/1753-6405.12166
19. McCormick, K., Salcedo, J. IBM SPSS Data Preparation. SPSS reg Statistics for Data Analysis and Visualization. 2017. Pp. 303–324. DOI: 10.1002/9781119183426.ch12

20. Pallant, J. SPSS survival manual: a step by step guide to data analysis using IBM SPSS. 2011. Pp. 597–598. DOI: 10.1046/j.1365-2648.2001.2027c.x
21. Field, A. Factor Analysis Using SPSS. Scientific Research and Essays. 2013. 22(6). Pp. 1–26. DOI: 10.1016/B978-0-444-52272-6.00519-5
22. Preacher, K.J., Hayes, A.F. SPSS and SAS procedures for estimating indirect effects in simple mediation models. Behavior Research Methods, Instruments, and Computers. 2004. 36(4). Pp. 717–731. DOI: 10.3758/BF03206553
23. Karpov, V.V., Semenov, A.A. Mathematical model of deformation of orthotropic reinforced shells of revolution. Magazine of Civil Engineering. 2013. 40(5). Pp. 100–106. DOI: 10.5862/MCE.40.11

Contacts:

Lina Zhang, 53860470@qq.com
Dongpo He, hdp@nefu.edu.cn
Qianqian Zhao, 492954791@qq.com